



IDENTIFICATION OF BENZIMIDAZOLE-TRIAZOLE HYBRIDS AS GLUCOSAMINE-6-PHOSPHATE SYNTHASE RECOGNITION THROUGH *IN SILICO* STUDIES

¹Uzma Khan, ²Hemlata Nimesh and ³Souvik Sur*

¹Department of Chemistry, Faculty of Engineering, Teerthanker Mahaveer University,
Moradabad, Uttar Pradesh-244001, India

²Amity Institute of Pharmacy, Amity University, Sector-125, Noida-201313, Uttar Pradesh,
India

³Research and Development Center, Teerthanker Mahaveer University, Moradabad, Uttar
Pradesh-244001, India

Corresponding author Email Address: drsouvik.engineering@tmu.ac.in

Abstract

This study presents a comprehensive *in silico* investigations of five benzimidazole-triazole hybrids (BPHT), checking their activity as Glucosamine-6-phosphate synthase inhibitors by means of molecular docking, ADMET assessment and normal mode studies. BPHT-3 showed the most beneficial docking score (-8.5), suggesting its binding affinity is strong. Based on ADMET screening, BPHT-3 shows good intestinal absorption, little risk to the heart and does not strongly affect certain liver enzymes. Data from normal mode analysis validated that despite being a bendable compound, BPHT-3 remains stable in interactions with the target enzyme since it obtained a very low eigen-value when connected to the target enzyme. In comparison to other derivatives, BPHT-3 gives the most balanced results for binding strength, how the drug gets into the body and flexibility in structure. With this approach, BPHT-3 is identified as a lead compound and researchers should now optimize it and perform experiments based on the importance of combining structural docking, pharmacokinetic modeling and molecular dynamics in early drug discovery.

Keywords: Molecular Docking, ADMET Profiling, Normal Mode Analysis, Glucosamine-6-phosphate Synthase, BPHT Derivatives

1. Introduction

The occurrence and widespread outbreak of fungal infections, particularly by opportunistic pathogens *Candida* and *Aspergillus*, is now of great concern all over the world.^{I-II} With more drug resistance developing in these pathogens, the effectiveness of many old-style antifungal treatments has fallen, leading to a strong desire for new approaches. To address this problem, scientists propose discovering new molecules and designing potent therapies against them. More and more attention has been given to Glucosamine-6-phosphate synthase (GlcN-6-P

synthase).^{III-V} For the fungal cell wall, the formation of chitin depends on UDP-N-acetylglucosamine and a pathway that starts by activating glucosamine with this enzyme forms chitin. Preventing the action of GlcN-6-P synthase stops cell wall formation in fungi, which leads to their death, but does not harm mammalian cells. Still, in light of all this, heterocyclic compounds are significant in medicinal chemistry thanks to their wide range of biologic activities and flexibility. Antimicrobial, antifungal, anti-inflammatory and anticancer properties are widely known for both benzimidazoles and triazoles scaffolds.^{VI-IX} Some have found that benzimidazole derivatives show effects on microtubules, DNA and enzymes, whereas triazoles, mostly 1, 2, 3-triazoles, are preferred for antifungal use because they inhibit cytochrome P450 enzymes in fungi. Mixing benzimidazole and triazole scaffolds may enrich the drug-like properties of a final compound, making these compounds stronger, more specific and safer than before. In this paper, we are examining the potential for new benzimidazole-triazole hybrids (**Figure 1**) to block GlcN-6-P synthase using various *in silico* tools and techniques.

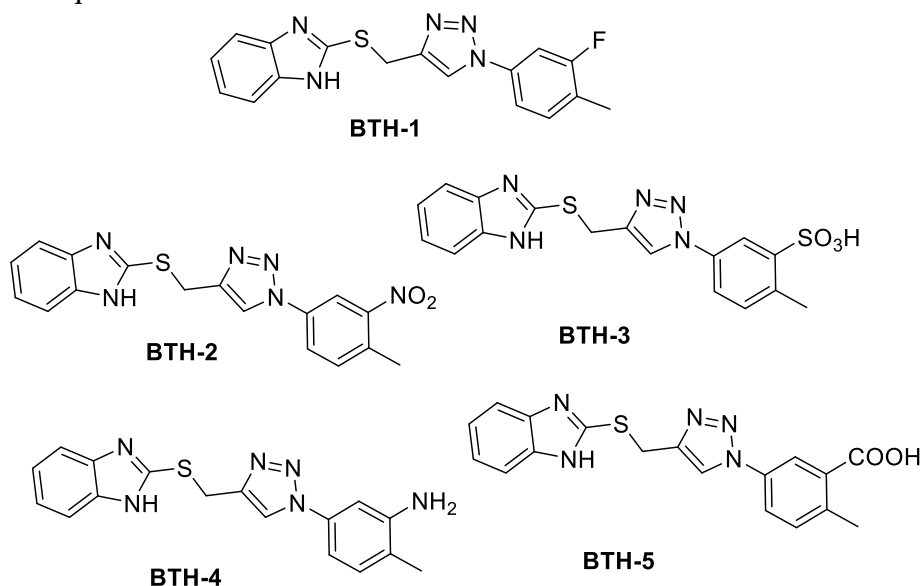


Figure 1: Structure of selected benzimidazole-triazole hybrids (BTH)

Computational studies start with docking, estimating interactions of the molecules with GlcN-6-P synthase before going on to assess their pharmacokinetics and how easily they can be used as drugs. Molecular dynamics simulations are also used to test the stability of the protein-ligand complexes over a period under normal body conditions to better understand their suitability for use as drugs. Using these tools together, we are looking to find hybrid molecules that are structurally good, attach effectively to important amino acid residues at the GlcN-6-P synthase site, have suitable tumor health and safety features and retain a stable shape. This system speeds up the first steps in drug discovery by doing less *in vitro* testing, as well as aids in choosing which candidates deserve to be synthesized and tested further.^X In short, the present study demonstrates a logical, structure-led approach using the synergy of benzimidazole and triazole structures to develop new antifungal medications. By providing new types of molecules that close this enzyme's active site, the results here may influence antifungal drug research and hopefully lead to better treatments for tough fungal infections.

Applying molecular docking and ADMET analyses at the same time strongly shapes the method used to improve benzo[h]quinoline derivatives for their function as DNA-interactive agents. By performing docking studies, we determine the compounds that interact best with

the target and perform an ADMET analysis to see how safe and suitable these compounds are. This combination of methods both speeds up the search for anticancer drugs and raises the chance of getting safe and effective results.

2. Experimental Methods:

2.1 Molecular Docking

Molecular docking experiment for the BTH-derivatives Glucosamine-6-phosphate synthase enzyme was performed using AutoDock,^{XI-XII} a well-known non-commercial docking programme. The structure of PDB was obtained from protein data bank (PDB ID. 2VF5).^{XIII} To enhance the thermodynamic stability of ligand attached to the enzyme more we used stochastic Lamarckian genetic algorithm-based docking strategy along with minimization of scoring function. We docked the following medications using AutoDock Vina 4.2. Intermediary tasks, such as generation of grid boxes as well as pdbqt files for both enzyme and ligands, were performed, using the Graphical User Interface programme AutoDock Tools (ADT). The targeted enzyme sequences contained polar hydrogens and Kollman charges were added to the sequences by the authors during the manual process. The first set of the targeted Files for enzyme and drugs were stored in formats with PDBQT extension. AutoGrid was employed for generation of the grid to be used in the grid map using grid box was and the dimensions were set to $50 \times 50 \times 50$ xyz points with a point spacing of 0.275 Å. The docked structures that were acquired were examined using Biovia Discovery Studio.^{XIV} The labelled amino acids, also known as the interacting residues, were in intimate contact with all three analogues. The presence of any potential interactions, such as H-bonding or other potential van der Waal interactions, in each docked complex was examined.

2.2 ADMET calculation

ADMET properties of all five BPHT-derivatives were calculated through <https://www.rowansci.com> platform.^{XV} The chemical structures of all five compounds were uploaded in SMILES format to get all the data.

2.3 Drug interaction analysis

iMODS (Integrated Molecular Dynamics Simulator) is the most reliable software used in simulation when working with docked complexes. iMODS outcomes are produced by normal mode analysis (NMA) applied to the protein-ligand docking systems.^{XVI} With iMODS, graphical methods are used to illustrate the stiffness properties of a challenging structure using deformability, eigenvalue, variance, covariance and elastic network models.


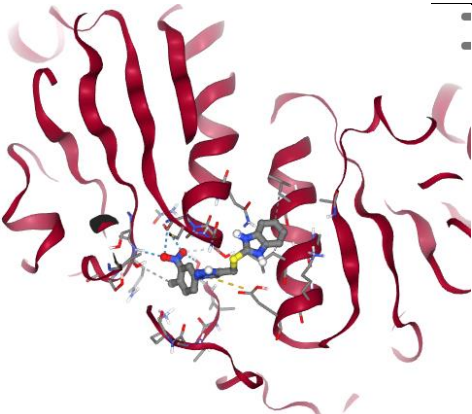
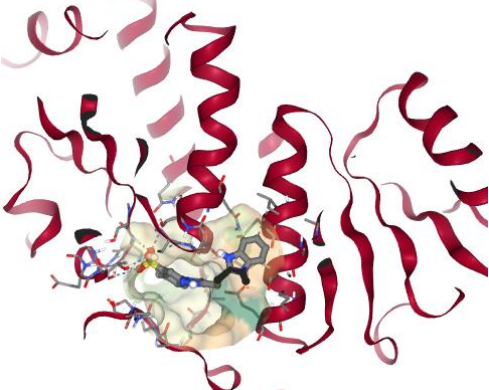
3. Result and Discussions

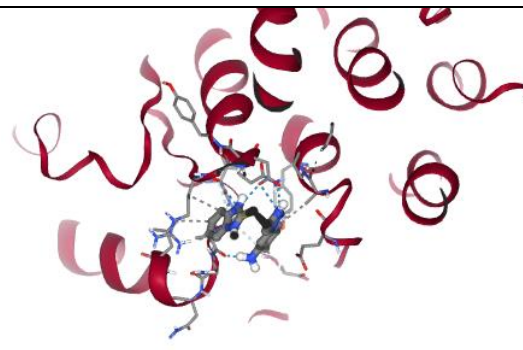
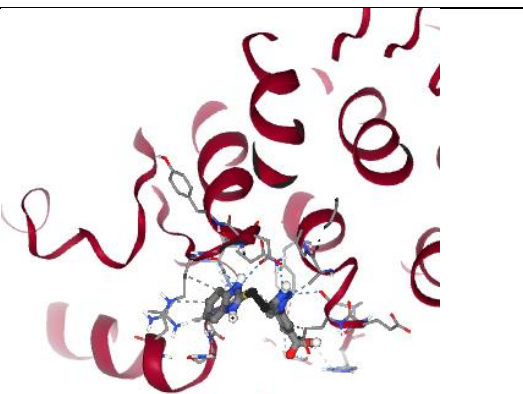
3.1 Molecular Docking

The results in the table show how various BPHT derivatives interact with the target enzyme, Glucosamine-6-phosphate synthase during the docking study. More negative docking scores in this study suggest a better predicted interaction between BPHT compounds and the target protein. Compound BPHT-3 showed the best binding properties, scoring -8.5 in the docking simulation. It seems likely that the reason for BPHT-3 being the most stable complex is that it forms better molecular bonds with Glucosamine-6-phosphate synthase than BPHT-2. The docking score of -8.1 for BPHT-5 put it in second place, then BPHT-2 at -8.0, BPHT-4 at -7.9 and BPHT-1 at the back with a score of -7.6. Researchers broke down the docking pose of BPHT-3 to see which amino acids in the active site are involved in binding the ligand. A study of this interaction map can reveal how binding occurs which may help scientists design improvements to the binding process. Many of these bonds which include hydrogen bonds,

hydrophobic interactions and electrostatic forces, help the enzyme to hold the ligand in its binding pocket. To design drugs more effectively, we need to discover these key residues to guide how we alter the molecules. It appears that BPHT-3 displays the most promising results for drug development, given how well it binds. The comparative nature of the docking scores across the BPHT series helps in prioritizing candidates for synthesis and biological evaluation. Moreover, the results highlight the value of molecular docking as a predictive tool in early-stage drug development, allowing researchers to focus resources on the most promising compounds. In summary, the docking study identifies BPHT-3 as the top-performing compound against Glucosamine-6-phosphate synthase, supporting its potential role in enzyme inhibition and setting a foundation for subsequent experimental validation and structure-activity relationship (SAR) studies.

Table 1: Molecular Docking Studies

Compound Entry	Docking Score*	3D Docked Pose
BPHT-1	-7.6	
BPHT-2	-8.0	
BPHT-3	-8.5	

BPHT-4	-7.9	
BPHT-5	-8.1	

*Docking scores are calculated in kcal mol⁻¹

Looking at the scores in comparison makes it easier to decide which molecules should be produced and examined biologically first. Besides, the study underlines why scientists rely on molecular docking early on, since it helps them choose the best compounds to study. Overall, the docking study shows that BPHT-3 is the most effective against Glucosamine-6-phosphate synthase which suggests it could play a role in inhibiting the enzyme and helps plan further experiments and SAR studies.

While analyzing, the docked structure of BPHT-3 with Glucosamine-6-phosphate synthase, it was found that key interactions explained by X-ray crystallography make its binding stronger and result in a much higher score of -8.5. There are two views on the screen-using 3D to show BPHT-3 in the enzyme's binding pocket and 2D to display in detail how the drug binds to the enzyme (**Figure 2**). Within the active site of the enzyme and surrounded by several crucial amino acid residues in the 3D panel, BPHT-3 fits well and is stabilized. The enzyme pocket has a see-through surface, so viewers can tell how accurately BPHT-3 fits into it. Clear stick models are used to illustrate the ligand, with the main functional and aromatic groups shown in positions for optimum interactions. Residues Cys300, Gly301, Glu348, Thr352 and Leu484 are found in the near proximity of the ligand. Among all, Glu348 and Thr352 establish hydrogen bonds with the polar end of the ligand, whereas Cys300 and Gly301 also provide stability by hydrogen bonding or van der Waals forces. Because Leu484 is hydrophobic, it probably interacts with the aromatic groups in BPHT-3 by π - π or alkyl binding which holds the molecule in place at the active site.

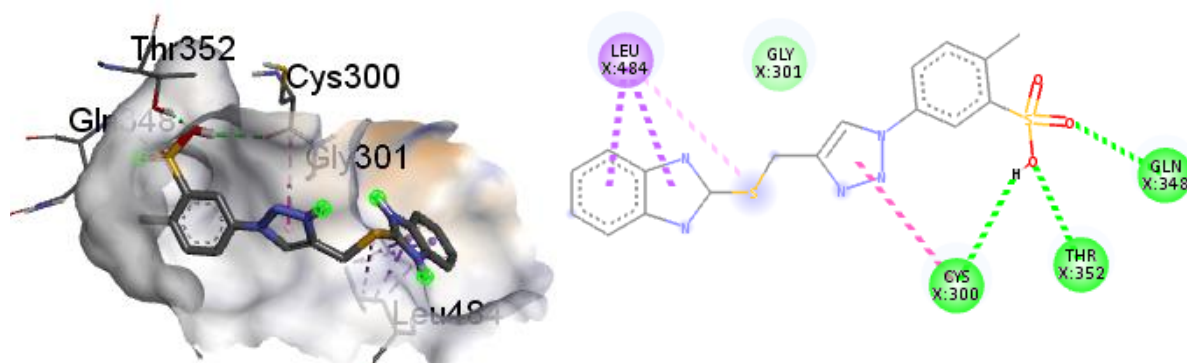


Figure 2: Docked structure of BPHT-3 with Glucosamine-6-phosphate synthase indicating interactive amino acids with ligand

These interactions are even easier to grasp when we look at the accompanying 2D interaction diagram. Various bonds and interactions are shown here by different colored dashed lines. Dashed lines of green highlight where the ligand connects to GLN348, THR352 and CYS300 by hydrogen bonds. This binding strength and specificity seen in BPHT-3 depend greatly on these interactions. The main reason ligand affinity is high is due to hydrogen bonding which helps the compound stay put in the active site of the enzyme. Having these bonds means BPHT-3 can secure the active site so that the enzyme cannot interact with its usual substrate. Pink and purple dashed lines mean π - π stacking and hydrophobic interactions, as can be seen between LEU484 and the aromatic parts of BPHT-3. Although van der Waals forces are not as strong as hydrogen bonds, they help to increase the number of places where a ligand touches the enzyme. There is evidence the residue GLY301 is close to the ligand, possibly interacts through its backbone and this enhances the stability and correct positioning of the compound.

3.2 ADMET Profiling

Pharmacokinetic behavior and safety information from ADMET testing gives key insights into the three compounds and their suitability as possible drug candidates. The three compounds all display significant human intestinal absorption (HIA) and oral bioavailability, as all their values are above 0.89. A lower level of permeability across the blood-brain barrier model was seen in BPHT-3, with values of 0.658 for BPHT-1 and 0.664 for BPHT-2. There is less oral absorption capability in BPHT-3, as indicated by the lowest F50 result of 0.403 out of BPHT-1, BPHT-2 and BPHT-3. The largest amount of distribution (VDss) seen is in BPHT-1 (0.31), a moderate volume is seen in BPHT-2 (0.021) and a significantly negative distribution is shown in BPHT-3 (-0.87). Thus, it seems that BPHT-3 may stick mostly to plasma and not spread into tissues as much. All three compounds have high PPB and BPHT-3 has the highest of all, suggesting strong attachment to plasma proteins that might interfere with its free drug level.

It is believed that multiple cytochrome P450 enzymes, particularly CYP1A2, CYP3A4 and CYP2C19, will be blocked by BPHT-1 and BPHT-2 but not by BPHT-3. BPHT-3's minimal interaction with metabolizing enzymes such as CYP3A4 and CYP2D6 suggests it could be metabolized differently than other types of drugs. Both HLM and RLM stability are greatest in BPHT-1 and BPHT-2, compared to BPHT-3 which may suggest that BPHT-3 breaks down or is cleared more quickly in the liver. Among the compounds, BPHT-3 (0.70) has the highest amount removed by the kidney, indicating it excretes faster through that organ. BPHT-3 has the lowest clearance via plasma (CL_{p_c}) of all, showing that it may leave the body slowly.

The toxicity of BPHT-3 cannot be easily summed up. At a concentration of 1 μ M, the product presents no risk to the heart which acts as a safety advantage because it does not make the QT intervals longer than normal. However, BPHT-3 results show increased respiratory and reproductive toxicity compared to the last version and this might be concerning. Also, it reveals that mitochondrial and hemolytic toxicity is much more prominent in PBOHT than in BPHT-1 and BPHT-2. The fact that BPHT-3 is predicted to be a UGT substrate (0.705) means it may be glucuronidated during metabolism. Although the ratings for carcinogenicity are not the same, mouse carcinogenicity for BPHT-3 is higher (0.837) but rodent carcinogenicity probabilities are lower. Based on how it affects the environment, BPHT-3 has less toxicity to water and lower bioaccumulation than BPHT-1 and BPHT-2.

Table 2: ADMET profiling data

Compound Entry	BPHT-1	BPHT-2	BPHT-3	BPHT-4	BPHT-5
TPSA	59.39	102.53	113.76	85.41	96.69
SlogP	3.88342	3.65252	2.99102	3.32652	3.44252
logS	-5.841113	-5.575976	-4.226638	-5.246975	-4.930673
QED	0.5732545	0.3284618	0.3902132	0.4409203	0.5259666
Lipinski_rule	Accept	Accept	Accept	Accept	Accept
Pfizer_rule	Not accept	Accept	Accept	Accept	Accept
GSK_rule	Accept	Accept	Not accept	Accept	Accept
logP	4.0835447	3.7667012	1.628363	3.6500545	3.1479087
pKa	5.0179315	4.2473693	3.7555583	6.1191897	4.7892175
HIA	0.9916761	0.9869594	0.8990049	0.9910642	0.9867214
MDCK	0.6581653	0.6648164	0.441692	0.5422601	0.4225084
F50	0.6901752	0.7389567	0.4038678	0.7182407	0.8725284
BBB	0.9478075	0.9230013	0.632633	0.9424431	0.6995953
OATP1B1_inhibitor	0.9399302	0.9104998	0.8728389	0.9362559	0.8386119
OCT1_inhibitor	0.792454	0.7578956	0.1399962	0.8247771	0.3298731
BCRP_inhibitor	0.5227678	0.5536049	0.269781	0.6529883	0.5672027
BSEP_inhibitor	0.946168	0.9540802	0.7358119	0.953258	0.8216755
MATE1_inhibitor	0.3269109	0.371253	0.0710276	0.3634305	0.1277657
Pgp_inhibitor	0.8874021	0.9278077	0.3879291	0.9302891	0.6918617
Pgp_substrate	0.2741773	0.327460	0.3996596	0.470601	0.268789

		9		6	7
PPB	0.9955131	0.949702 6	1.0127568	0.984123 8	0.975854 9
VDss	0.3115773	0.021215 1	-0.870684	0.182848	-0.604656
CYP1A2_inhibitor	0.989628	0.978486 8	0.2340784	0.986612 3	0.697408 3
CYP3A4_inhibitor	0.8825921	0.913714 3	0.2185643	0.903906 2	0.304737 4
CYP2B6_inhibitor	0.7231513	0.730377 5	0.1236559	0.747897 4	0.227158 1
CYP2C9_inhibitor	0.8727185	0.886879 7	0.565363	0.864074 6	0.669164 8
CYP2C19_inhibitor	0.95335	0.951647 7	0.3615128	0.948234 4	0.471262 9
CYP2D6_inhibitor	0.7597359	0.760640 6	0.0579202	0.765748 8	0.097324 3
CYP1A2_substrate	0.8995318	0.916779 2	0.3051443	0.907512 3	0.552301 1
CYP3A4_substrate	0.7491898	0.817513 9	0.4879538	0.734821 8	0.477812 1
CYP2B6_substrate	0.635373	0.612940 1	0.1330998	0.593613 9	0.173182 8
CYP2C9_substrate	0.6276714	0.746361 6	0.5407385	0.626145 5	0.644763 1
CYP2C19_substrate	0.8121961	0.861366 6	0.3575247	0.797335 3	0.552156 2
CYP2D6_substrate	0.6164811	0.704407 3	0.1408395	0.736700 2	0.192825 9
HLM	0.7557239	0.796983 5	0.1199342	0.779787 6	0.196673
RLM	0.8806081	0.890060 5	0.2093268	0.915534 6	0.332769
UGT_substrate	0.2515036	0.202107 2	0.705846	0.262976 2	0.766157 3
CLp_c	0.6599903	0.592976 9	0.2960816	0.682237 6	0.215343 6
CLr	0.537223	0.539584 8	0.702698	0.577272 7	0.707988
T50	-1.173831	-1.185313	0.1224657	-0.963281	-0.505691
MRT	-1.16544	-1.172131	0.2823725	-0.959747	-0.483131
Neurotoxicity	-2.415015	-2.411307	-2.760699	-2.387058	-2.946465
DILI	0.7394993	0.758522 9	0.5893906	0.705773 2	0.839263 7
hERG_1uM	0.2704858	0.267980 1	0.0037338	0.474137	0.010247
hERG_10uM	0.9518411	0.926045 3	0.4867868	0.979142 2	0.486160 4

hERG_30uM	0.9935633	0.987932	0.9101688	0.9962423	0.9391313
hERG_1_10uM	0.8018796	0.7641652	0.0114977	0.9347484	0.0308685
hERG_10_30uM	0.9935808	0.9873477	0.8097909	0.9971457	0.8614805
Respiratory_toxicity	0.4693838	0.3676861	0.974986	0.620277	0.9308634
Nephrotoxicity	0.5658007	0.6020491	0.360494	0.426989	0.4603418
Eye_corrosion	0.0167487	0.0169712	0.00042	0.0109914	0.0003606
Eye_irritation	0.4563664	0.4345336	0.0036701	0.3572413	0.0135041
Skin_corrosion	0.0159233	0.0140001	0.0050126	0.0236044	0.0038194
Skin_irritation	0.0824951	0.0653082	0.0878968	0.1137228	0.0726326
Skin_sensitisation	0.1196521	0.0766103	0.0193614	0.1026516	0.0284943
ADT	0.6942312	0.7393303	0.7389113	0.7060474	0.7515793
Ames	0.9085663	0.953833	0.2774443	0.9273764	0.7287186
Mouse_carcinogenicity_c	0.6512341	0.696559	0.2673472	0.6636633	0.5733538
Mouse_carcinogenicity	0.5709215	0.2777163	0.8377605	0.124812	0.68254
Rat_carcinogenicity_c	0.5067626	0.5676713	0.4558823	0.522912	0.621843
Rat_carcinogenicity	1.4401991	1.3383893	1.6219373	1.0753198	1.3941772
Rodents_carcinogenicity	0.6590426	0.7240019	0.3014559	0.6979374	0.6428674
Micronucleus	0.9318878	0.9495867	0.8256692	0.9208593	0.9088593
Reproductive_toxicity	0.7022005	0.6749082	0.9655287	0.71876	0.8827626
Mitochondrial_toxicity	0.9158226	0.9223984	0.0689196	0.8811083	0.2710795
Hemolytic_toxicity	0.0486835	0.0465958	0.5053141	0.0649964	0.116674
Repeated_dose_toxicity	0.881583	0.8829066	0.5189652	0.8635209	0.6109959
AOT_c	0.8034913	0.860658	0.6657858	0.8720368	0.8217205
AOT	-3.16837	-2.931828	-2.831996	-3.110959	-2.792925
FDAMDD_c	0.6135091	0.636381	0.8288568	0.736549	0.548343

		9		3	5
FDAMDD	2.1961617	2.142665 4	2.806633	2.294411 2	2.274955 5
AR	0.3598468	0.457937 4	0.0750892	0.295063 3	0.112266 9
ER	0.3042611	0.346296 3	0.0181691	0.261293 6	0.047794 2
AR_LBD	0.4070596	0.445375 6	0.0687862	0.335337 1	0.098577 5
ER_LBD	0.6385279	0.635375 4	0.0393655	0.555592 9	0.134615
Aromatase	0.7018595	0.686478 7	0.1470141	0.603256 9	0.254856 3
AhR	0.9091468	0.908631 3	0.1462296	0.920230 9	0.559612 1
ARE	0.8560761	0.878902 9	0.067435	0.859290 1	0.328542 4
ATAD5	0.3471278	0.386338 2	0.0225301	0.442638 4	0.116279 1
HSE	0.3700716	0.389563 5	0.0080652	0.382106 7	0.043843
p53	0.6220878	0.687931 8	0.0192217	0.606311 5	0.143389 2
PPAR	0.4218398	0.51881	0.089336	0.443690 7	0.324290 4
MMP	0.9147993	0.935933 8	0.0181699	0.884750 2	0.242197 3
TR	0.6235672	0.637469 4	0.0538093	0.566048 1	0.326093
GR	0.45507	0.458679	0.110107	0.390509 5	0.207975 6
subcapitata_toxicity	0.8903229	0.828724 4	0.5106073	0.861239 1	0.735019 6
Crustaceans_toxicity	0.9133205	0.911338 3	0.1683644	0.888057 6	0.296439 4
magna_toxicity	0.9132125	0.913629 7	0.1687324	0.888813 6	0.307877 8
Fish_toxicity	0.9108243	0.90365	0.4715351	0.824091	0.352531 4
Fathead_minnow_toxicity	0.8563278	0.838785 6	0.2870056	0.768771 3	0.310257 3
Bluegill_sunfish_toxicity	0.9461008	0.945542 5	0.2806317	0.911069 6	0.312496
Rainbow_trout_toxicity	0.9496453	0.948310 4	0.3883018	0.901956 6	0.390584 1
Sheepshead_minnow_toxicity	0.9494095	0.943766 7	0.3262334	0.912849 1	0.569679 4
pyriformis_toxicity_c	0.997104	0.995123	0.8943841	0.994334	0.965163

					6
pyriformis_toxicity	1.9508135	1.770376 2	0.2079826	1.747200 3	0.860029 3
Honey_bee_toxicity	0.1146724	0.136548 4	0.0566889	0.120927 3	0.031839 8
Colinus_virginanus_toxicity	0.165849	0.218743 1	0.056122	0.159187 2	0.038116 2
Anas_platyrhynchos_toxicity	0.0878206	0.114810 5	0.0437795	0.080565 7	0.029307 2
BCF_c	0.2759666	0.301751 8	0.0202632	0.196819 1	0.023573 6
BCF	2.4448214	2.289231 8	0.7942891	2.217075 1	0.650694 4
Biodegradability	0.0254385	0.020516 6	0.0924328	0.029826	0.043790 2
Photoinduced_toxicity	0.726708	0.713820 9	0.5944515	0.734453 9	0.797964 3
Phototoxicity_Photoirritation	0.5983813	0.599044	0.2706231	0.637635 1	0.525210 3
Photoallergy	0.6592223	0.636814 7	0.5677673	0.651615 7	0.753573 1

In summary, BPHT-3 looks favorable for heart and metabolic interactions, but its lower absorption, less tissue reach and special concerns with the mitochondria, respiratory system and reproductive system point to the need for extra optimization. The limited CYP inhibition and differing ways it is removed from the body may mean this molecule can be further developed and its toxicity lowered.

3.3 Drug interaction analysis

The iMod simulation study provides comprehensive results related to structural deformity, eigenvalues, and heat maps, which are critical for understanding protein dynamics.

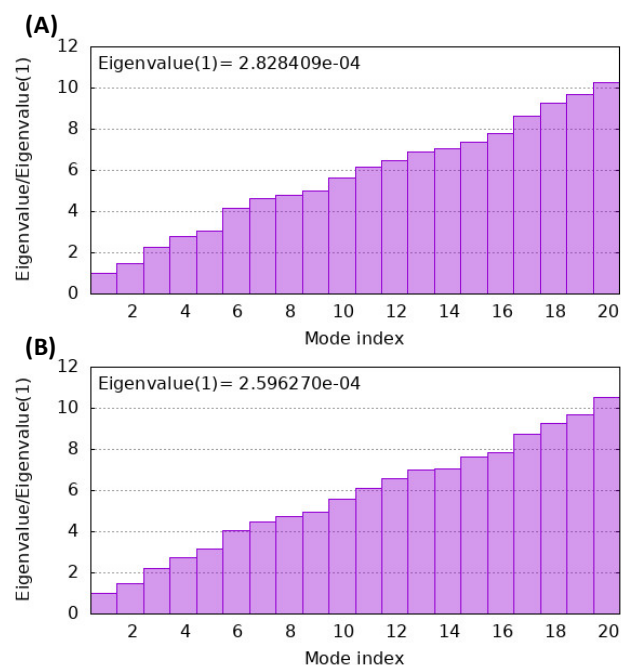


Figure 3: Molecular dynamics simulation results for (A) Glucosamine-6-phosphate synthase and (B) BPHT-3 docked Glucosamine-6-phosphate synthase by iMOD eigen value map

We used the iMod online server to make these findings even better and more accurate. All the results shown in iMod, including those for structural deformity, eigen-values and heat maps, highlight essential aspects of protein dynamics. The graph (**Figure 3**) presents two bar charts illustrating normalized eigen-values from normal mode analysis (NMA) for a range of vibration modes. NMA is commonly employed to evaluate the flexibility of proteins or systems when there is a ligand present. Both graphs use the mode index on their x-axis and show eigen-values normalized to the first mode on the y-axis. How much energy is needed to move the structure in each vibrational way is shown by its eigenvalues. Materials with low eigen-values can be shaped more easily without investing much energy. For the graph at the top, the first mode contains an eigen-value of 2.828409e-04 and in the bottom graph, it is 2.596270e-04. This demonstrates that the bottom structure can move more freely in its lowest vibrational state than the top one. The straight and slow increase in eigen-values on the graphs points to the fact that higher modes are more rigid. The even spread of eigen-values suggests a well-distributed motion range and the important; slow-speed movements for living functions are mainly controlled by lower modes. Since the ability to change shape is important for molecules to connect with and recognize other molecules, the mark on the y-axis at the bottom tells us that such changes are feasible for this structure. The ability to change shapes may help drugs to attach to a target more efficiently during drug discovery.

4. Conclusion

Using molecular docking, ADMET profiling and normal mode analysis, we studied BPHT derivatives, focusing especially as likely inhibitors of Glucosamine-6-phosphate synthase. BPHT-3 was the best performer among the tests, with a docking score of -8.5 which suggests a strong attachment to the target enzyme. Many supporting contacts, including hydrogen bonds and hydrophobic links involving Cys300, Gly301, Thr352 and Glu348 amino acids, were observed during the interaction analysis, suggesting the compound can be considered a lead candidate. By performing ADMET screening on BPHT-3, we observed that it is taken up

well by the intestine and barely reaches the brain. Yet, BPHT-3 suffered from some pharmacokinetic drawbacks such as being metabolically unstable and having worries about toxicity to mitochondria and the reproductive system. There were very few effects on cytochrome P450 enzymes which may lower the risk of drug interactions in the body. Additionally, it is known to have a low risk of damaging the heart because it does not affect the important hERG channel. The results from normal mode analysis suggest that BPHT-3 forms a secure but adaptable bond with the enzyme which is beneficial for good molecular binding. When placed alongside other alternatives, BPHT-3 showed the greatest strengths for binding rate, flexibility and basic pharmacokinetic properties.

Overall, BPHT-3 is the leading candidate among the derivatives examined in this study. Although the drug displays firm interactions and acceptable ADMET scores, certain toxicity risks indicate the need for further changes. Integrating docking, ADMET and analyzing flexibility shows that a multi-parametric method is beneficial in the initial drug testing and BPHT-3 has the potential to be further developed and tested experimentally.

Financial support

This research did not receive any funding.

Conflicts of interest

The authors have no conflicts of interest.

Reference

- I. Pfaller, M. A., & Diekema, D. J. (2004). Rare and emerging opportunistic fungal pathogens: concern for resistance beyond *Candida albicans* and *Aspergillus fumigatus*. *Journal of clinical microbiology*, 42(10), 4419-4431.
- II. Gnat, S., Łagowski, D., Nowakiewicz, A., & Dyląg, M. (2021). A global view on fungal infections in humans and animals: opportunistic infections and microsporidiosis. *Journal of Applied Microbiology*, 131(5), 2095-2113.
- III. Milewski, S. (2002). Glucosamine-6-phosphate synthase—the multi-facets enzyme. *Biochimica et Biophysica Acta (BBA)-Protein Structure and Molecular Enzymology*, 1597(2), 173-192.
- IV. Wojciechowski, M., Milewski, S., Mazerski, J., & Borowski, E. (2005). Glucosamine-6-phosphate synthase, a novel target for antifungal agents. Molecular modelling studies in drug design. *Acta Biochimica Polonica*, 52(3), 647-653.
- V. Teplyakov, A., Obmolova, G., Badet-Denisot, M. A., & Badet, B. (1999). The mechanism of sugar phosphate isomerization by glucosamine 6-phosphate synthase. *Protein Science*, 8(3), 596-602.
- VI. Marinescu, M. (2023). Benzimidazole-triazole hybrids as antimicrobial and antiviral agents: A systematic review. *Antibiotics*, 12(7), 1220.
- VII. Khan, Y., Rehman, W., Hussain, R., Khan, S., Malik, A., Khan, M. & Abdellatif, M. H. (2022). New biologically potent benzimidazole-based-triazole derivatives as acetylcholinesterase and butyrylcholinesterase inhibitors along with molecular docking study. *Journal of Heterocyclic Chemistry*, 59(12), 2225-2239.
- VIII. Singh, D. K., Iqbal, H., & Ansari, M. A. (2024). Recent Progress in the Synthesis and Biological Assessment of Benzimidazole-1, 2, 3-Triazole Hybrids. *Current Organic Chemistry*, 28(10), 733-756.
- IX. Tahlan, S., Kumar, S., & Narasimhan, B. (2019). Pharmacological significance of heterocyclic 1 H-benzimidazole scaffolds: a review. *BMC chemistry*, 13, 1-21.

- X. Soliman, M. A., Ahmed, H. E., Eltamany, E. H., Boraei, A. T., Aljuhani, A., Salama, S. A., ... & Aouad, M. R. (2025). Novel bis-benzimidazole-triazole hybrids: anticancer study, in silico approaches, and mechanistic investigation. *Future Medicinal Chemistry*, 17(1), 93-107.
- XI. Huey, R., Morris, G. M., & Forli, S. (2012). Using AutoDock 4 and AutoDock vina with AutoDockTools: a tutorial. *The Scripps Research Institute Molecular Graphics Laboratory*, 10550(92037), 1000.
- XII. Tanchuk, V. Y., Tanin, V. O., Vovk, A. I., & Poda, G. (2016). A new, improved hybrid scoring function for molecular docking and scoring based on AutoDock and AutoDock Vina. *Chemical biology & drug design*, 87(4), 618-625.
- XIII. Mouilleron, S., Badet-Denisot, M. A., & Golinelli-Pimpaneau, B. (2008). Ordering of C-terminal loop and glutaminase domains of glucosamine-6-phosphate synthase promotes sugar ring opening and formation of the ammonia channel. *Journal of molecular biology*, 377(4), 1174-1185.
- XIV. Sharma, S., Sharma, A., & Gupta, U. (2021). Molecular Docking studies on the Anti-fungal activity of *Allium sativum* (Garlic) against Mucormycosis (black fungus) by BIOVIA discovery studio visualizer 21.1. 0.0. *Annals of Antivirals and Antiretrovirals*, 5(1), 028-032.
- XV. Swanson, K., Walther, P., Leitz, J., Mukherjee, S., Wu, J. C., Shivnaraine, R. V., & Zou, J. (2024). ADMET-AI: a machine learning ADMET platform for evaluation of large-scale chemical libraries. *Bioinformatics*, 40(7), btae416.
- XVI. López-Blanco, J. R., Garzón, J. I., & Chacón, P. (2011). iMod: multipurpose normal mode analysis in internal coordinates. *Bioinformatics*, 27(20), 2843-2850.

Received on May 27, 2025.